

Three-Dimensional Optimum Thrust Trajectories for Power Limited Propulsion Systems

WILLIAM G. MELBOURNE¹

Jet Propulsion Laboratory
Pasadena, Calif.

The three-dimensional equations for optimum variable thrust with power limited propulsion systems are presented. An iterative routine for solving the two-point boundary value problem has been coupled with these equations to obtain numerical solutions for specified end conditions. A set of interplanetary rendezvous trajectories to Venus and Mars is presented, and the effects of orbital inclination and eccentricity are assessed.

FOR THE past few years mission feasibility studies and trajectory analyses have been conducted to assess the payload capabilities of power limited advanced propulsion vehicles for various interplanetary missions. This paper describes one type of optimum thrust program for power limited propulsion systems which is currently being used in these studies.

The power limited propulsion system is constrained in the amount of kinetic power contained in the exhaust propellant. By a consideration of the energy and momentum equations, a rocket equation suitable for such a system is obtained. This is given by

$$\frac{1}{m_1} = \frac{1}{m_0} + \int_0^{t_1} \frac{a^2}{2P} dt \quad [1]$$

where m_0 and m_1 are the vehicle masses at the beginning and end, respectively, of the flight, a is the thrust acceleration, and P the power expended in the rocket exhaust. The exhaust power is determined by the power rating of the power plant carried by the vehicle and by the efficiency of conversion by the propulsion system, which is generally dependent on the exhaust velocity. The final vehicle mass depends on the value of this integral, which in turn depends on the flight time, the mission involved (namely, the specification of the kinematic conditions of the vehicle initially and terminally), the force field in which the vehicle travels, the nature of the thrust program used to accomplish this mission, and finally, the engineering design of the propulsion system. This integral is analogous to the concept of incremental velocity in a chemical rocket and is useful in payload optimization studies.

For the preliminary mission feasibility studies, it is desirable to employ optimum thrust programs which exclude the complexity imposed by the engineering design but which bracket or isolate that class of trajectories and vehicle performances which an actual vehicle would be capable of achieving.

One such thrust program, which partially fulfills this need, is obtained by satisfying the criterion that the quantity $\int_0^{t_1} a^2 dt$ is a minimum using an unconstrained thrust magnitude and direction. The justification of this program is based on the fact that over a wide range of specific impulse,

but excluding lower values, the power conversion efficiency of the propulsion system is nearly constant, thus allowing the removal of P from the integral. Since the thrust is unconstrained, this program yields the absolute minimum that $\int_0^{t_1} a^2 dt$ may have for a given mission and therefore leads to a somewhat optimistic estimate of vehicle payload.²

The equations of motion of a vehicle in a conservative force field may be written in vectorial form as

$$\ddot{\mathbf{r}} + \nabla V - \mathbf{a} = 0 \quad [2]$$

where \mathbf{r} is the position vector and V the potential in this force field. The minimization of $\int_0^{t_1} a^2 dt$ may be accomplished by calculus of variations methods in which this integral is minimized subject to certain constraints, namely, the equations of motion and the initial and terminal kinematic conditions specified by the mission.

For the variable thrust program, it may be shown (1-3)³ that the thrust acceleration equations that must be satisfied as necessary conditions for minimum $\int_0^{t_1} a^2 dt$ are the Euler-Lagrange equations

$$\ddot{\mathbf{a}} + (\mathbf{a} \cdot \nabla) \nabla V = 0 \quad [3]$$

Since V is not an explicit function of time, these equations admit a first integral in scalar form which may be expressed as

$$\dot{\mathbf{a}} \cdot \dot{\mathbf{r}} - (1/2)a^2 + \mathbf{a} \cdot \nabla V = \text{const} \quad [4]$$

The present studies employ an inverse-square central force field model in three dimensions. Because of the spherical symmetry of this problem, it is advantageous to express these equations in spherical coordinates. This coordinate system and the direction of the basis vectors are illustrated in Fig. 1. The state variables for this formulation are r , θ , ϕ , u , h_θ , and h_ϕ , where u is radial velocity, and h_θ and h_ϕ are the components of angular momentum per unit mass. The control variables are a_r , a_θ , and a_ϕ . After some manipulation it may be shown that Eqs. 2 and 3 may be expressed as

$$\dot{u} - (h^2/r^3) + (\mu/r^2) - a_r = 0 \quad [5]$$

² For a comparison of this program with a constant thrust program, consult Ref. 3.

³ Numbers in parentheses indicate References at end of paper.

Received April 26, 1961.

¹ Research Group Supervisor. Member ARS.

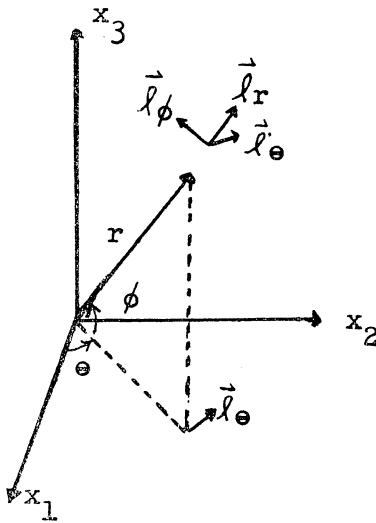


Fig. 1 Spherical coordinate system

$$u - \dot{r} = 0 \quad [6]$$

$$\dot{h}_\theta - (h_\phi^2 \tan \phi / r^2) + r a_\phi = 0 \quad [7]$$

$$\dot{h}_\phi + (h_\theta h_\phi \tan \phi / r^2) - r a_\theta = 0 \quad [8]$$

$$h_\theta + r^2 \dot{\phi} = 0 \quad [9]$$

$$\dot{h}_\phi - r^2 \dot{\theta} \cos \phi = 0 \quad [10]$$

$$\dot{h}^2 = \dot{h}_\phi^2 + \dot{h}_\theta^2 \quad [11]$$

$$\ddot{a}_r + \frac{3a_r}{r^4} \left[h^2 - \frac{2\mu r}{3} \right] - \frac{1}{r} [a_\theta^2 + a_\phi^2] - \frac{2h_\phi \tan \phi}{r^4} (\mathbf{h} \cdot \mathbf{a}) - \frac{h_\theta F(t)}{r^3} - \frac{K_1 h_\phi}{r^3 \cos \phi} = 0 \quad [12]$$

$$F(t) + 2r^2 \frac{d}{dt} \left[\frac{a_\phi}{r} \right] - \frac{4h_\theta a_r}{r} + \frac{2h_\phi a_\theta \tan \phi}{r} = 0 \quad [13]$$

$$\dot{F}(t) - \frac{2h_\phi}{r^3 \cos^2 \phi} (\mathbf{h} \cdot \mathbf{a}) - \frac{K_1 h_\phi \sin \phi}{r^2 \cos^2 \phi} = 0 \quad [14]$$

$$r^2 \frac{d}{dt} \left[\frac{a_\theta}{r} \right] + \frac{h_\phi}{r} (2a_r - a_\phi \tan \phi) - \frac{\tan \phi}{r} (\mathbf{h} \cdot \mathbf{a}) - \frac{K_1}{2 \cos \phi} = 0 \quad [15]$$

where h is the angular momentum per unit mass of the vehicle and μ the gravitational constant of the central body. The quantity $F(t)$ is an auxiliary variable, essentially one of the Lagrange multipliers that could not easily be eliminated. The constant K_1 is a constant of integration resulting from the cyclic nature of the variable θ . Eq. 4 becomes

$$a^2 - 2\dot{a}_r \dot{r} + \frac{2a_r}{r^3} [h^2 - \mu r] - \frac{K_1 h_\phi}{r^2 \cos \phi} - \frac{h_\theta F(t)}{r^2} - \frac{2h_\phi \tan \phi}{r^3} (\mathbf{h} \cdot \mathbf{a}) = K_2 \quad [16]$$

The quantities K_1 and K_2 are the only constants of motion which have been found. Eq. 16 is not used in numerical integrations because of the $\dot{a}_r \dot{r}$ term, but it is useful in checking the accuracy of the numerical integrations of Eqs. 5-15. It may be easily verified that these equations reduce to those contained in (1) upon reduction to two dimensions.

Missions and Terminal Conditions

The kinematic variables in most missions are specified at the initial point of a trajectory, and in a final trajectory design the terminal values are usually specified. In a preliminary study, however, it is advantageous to let certain terminal variables be free in order to optimize the trajectory with respect to certain criteria such as payload capability, communication distance, and error sensitivity.

In planetary rendezvous missions, six terminal quantities must be specified. It is convenient to group these into five quantities that determine the shape and orientation of the terminal orbit and one quantity indicating the rendezvous position on the orbit. These quantities are the energy per unit mass E , the angular momentum per unit mass h , the orbital inclination i , the argument of perigee ω , the longitude

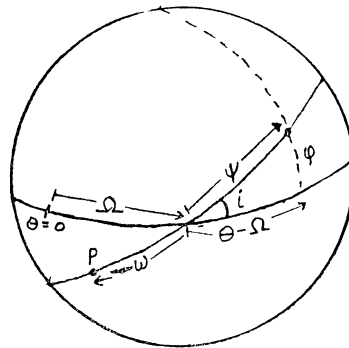


Fig. 2 Orbital elements

Table 1 Useful combinations of rendezvous terminal conditions and corresponding transversality relations^a

	I	II	III	IV	V	VI
1	$E = E_s$	$E = E_s$	$E = E_s$	$E = E_s$	$E = E_s$	$E = E_s$
2	$h = h_s$	$h = h_s$	$h = h_s$	$h = h_s$	$h = h_s$	$h = h_s$
3	$i = i_s$	$i = i_s$	$i = i_s$	$i = i_s$	$i = i_s$	$K_1 = 0$
4	$\omega = \omega_s$	$\omega = \omega_s$	$\omega = \omega_s$	$\Omega = \Omega_s$	$K_1 = 0$	$M = 0$
5	$\Omega = \Omega_s$	$\Omega = \Omega_s$	$K_1 = 0$	$M = 0$	$M = 0$	$\mathbf{a} \cdot \mathbf{h} = 0$
6	$\psi = \psi_s$	$M + N + \frac{K_1 h_\phi}{r^2 \cos \phi} = 0$	$M + N = 0$	$N + \frac{K_1 h_\phi}{r^2 \cos \phi} = 0$	$N = 0$	$F = 0$

^a The subscript s denotes a specified terminal value. The functions M and N are given by

$$M(t) = 2\dot{a}_r \dot{r} + (2a_r / r^3)(\mu r - h^2)$$

$$N(t) = [2h_\phi (\mathbf{a} \cdot \mathbf{h}) / r^3] \tan \phi + (h_\theta F(t) / r^2)$$

and will be recognized as components of Eq. 16.

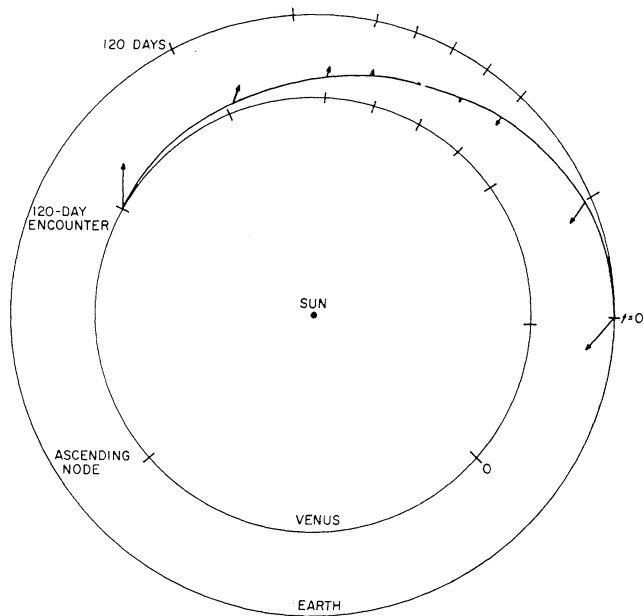


Fig. 3 Venus three-dimensional optimum rendezvous trajectory, ecliptic projection

of the ascending node Ω , and the angle from the line of nodes to the rendezvous point ψ . The angular quantities are exhibited in Fig. 2. These quantities are expressed in terms of the six kinematic variables through the relations

$$E = (1/2)[\dot{r}^2 + (h^2/r^2)] - \mu/r \quad [17]$$

$$h^2 = h_\theta^2 + h_\phi^2 \quad [18]$$

$$\cos i = h_\phi \cos \phi / h \quad 0 \leq i \leq \pi \quad [19]$$

$$\omega = \psi - \sin^{-1}(h\dot{r}/\mu e) \quad 0 \leq \omega \leq 2\pi \quad [20a]$$

$$\omega = \psi - \cos^{-1}\left[\frac{1}{e} \frac{h^2}{\mu r} - 1\right] \quad 0 \leq \omega \leq 2\pi \quad [20b]$$

$$\sin \Omega = \frac{-h_\theta \sin \theta - h_\phi \sin \phi \cos \theta}{h \sin i} \quad 0 \leq \Omega \leq 2\pi \quad [21a]$$

$$\cos \Omega = \frac{-h_\theta \cos \theta + h_\phi \sin \phi \sin \theta}{h \sin i} \quad 0 \leq \Omega \leq 2\pi \quad [21b]$$

$$\sin \psi = \sin \phi / \sin i \quad 0 \leq \psi \leq 2\pi \quad [22a]$$

$$\cos \psi = -h_\theta \cos \phi / h \sin i \quad 0 \leq \psi \leq 2\pi \quad [22b]$$

where e is the eccentricity of the ellipse. These six expressions may serve as boundary conditions at the terminal point of the trajectory. For each one of these conditions that is left unspecified, there is, from the calculus of variations, a corresponding transversality expression to be satisfied at the terminal point. Satisfying these transversality expressions yields extremals in the quantity to be optimized with respect to the unspecified boundary conditions. Both relative maxima and minima result from satisfying these conditions. The general formulation of transversality conditions may be found in treatises on calculus of variations; in (3) a formulation that is directly applicable to this problem is presented.

Table 1 lists several useful combinations of rendezvous terminal conditions and corresponding transversality relations obtained from an application of this formulation for a fixed final time. Combination I is, of course, the case where all six terminal conditions are specified. In combination II the position on the terminal orbit ψ is left unspecified, and the corresponding transversality condition appears. In combination III both ψ and Ω are unspecified, and two transversality

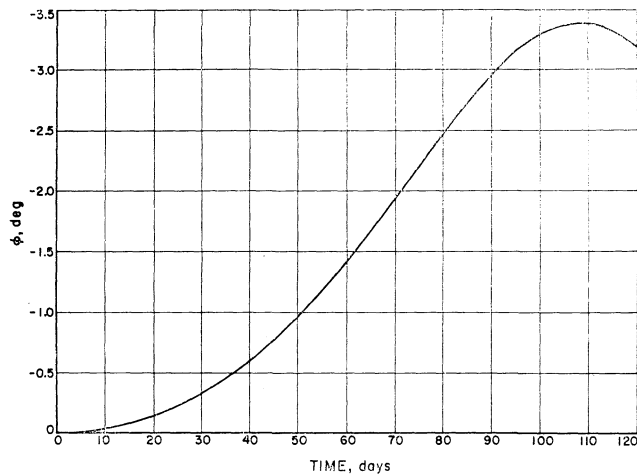


Fig. 4 Venus three-dimensional optimum rendezvous trajectory, celestial latitude

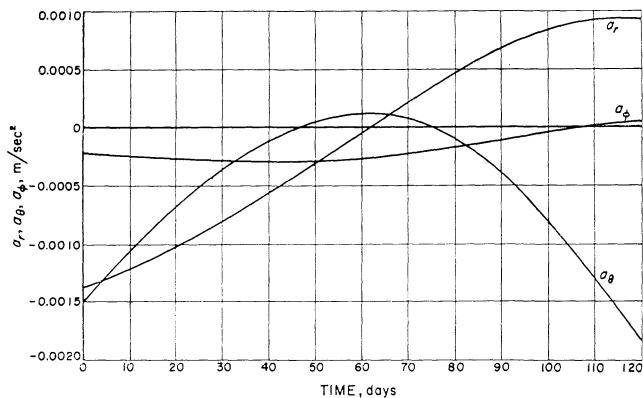


Fig. 5 Venus three-dimensional optimum rendezvous trajectory, thrust program

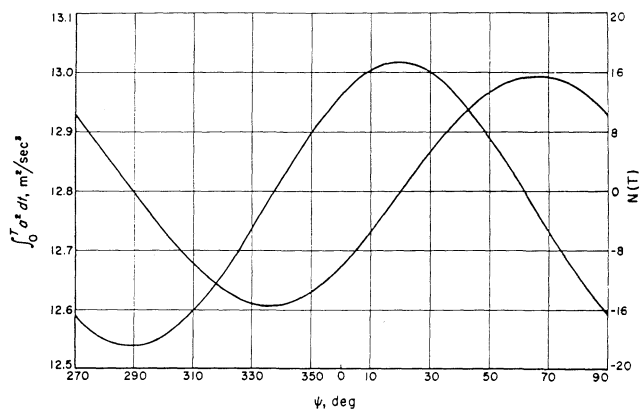


Fig. 6 Venus three-dimensional rendezvous trajectories, 120-day flight time

conditions result. This combination is most useful when the trajectory commences from a circular orbit, thus relaxing the necessity of specifying $\Omega(t_1)$. Combinations IV and V apply to circular terminal orbits and to the case of orbital inclination changes. Combination VI also applies to the two-dimensional case where $\mathbf{a} \cdot \mathbf{h}$ and $F(t)$ are zero over the trajectory. This

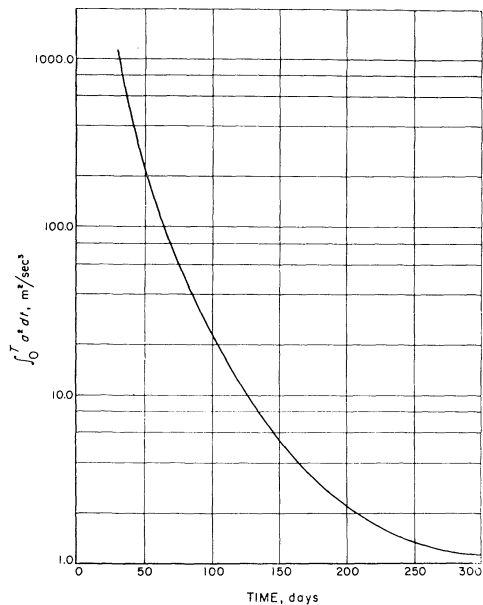


Fig. 7 Venus two-dimensional rendezvous trajectories

particular case has, in effect, been noted by Blum (1). The quantity K_1 is zero when neither θ nor any quantity explicitly dependent on θ , e.g., Ω , is specified.

Interplanetary Trajectories

In three dimensions, the set of equations to be solved requires the specification of 12 constants of integration. The specification of the six state variables initially and the six terminal and transversality conditions define the system.

D. E. Richardson of Jet Propulsion Laboratory has programmed these equations in an inverse-square force field for numerical solution on an IBM 7090 digital computer. To overcome the two-point boundary value problem associated with this type of equations, an iterative routine designed to efficiently conduct parametric analyses has been developed. Eqs. 5-15 are used to obtain a search matrix by a direct perturbation procedure. From this matrix a set of corrections to the initial conditions is obtained yielding a trajectory whose terminal conditions converge toward the specified values. The validity of this procedure is predicated on the assumption of a near-linear behavior of the variables in the small. Several devices are used to minimize computer time. If successive iterations are required, the original matrix is used as long as the process converges and the number of iterations is less than some specified value. To use this computer efficiently, a family of converged trajectories (for different terminal conditions and/or flight times, for example), is obtained in one machine run. This allows the accumulation of information about previously converged trajectories, which is used to predict initial conditions and search matrix elements for the succeeding case. This routine has been remarkably successful in the large-scale production of interplanetary rendezvous and flyby trajectories to nearly all the planets, with flight times ranging from 30 days to 3 years (2,3).

The numerical examples presented consist of sets of interplanetary rendezvous trajectories commencing from Earth's heliocentric position and terminating at Venus and at Mars. The orbits of Earth and Venus were assumed circular with the latter possessing an inclination of $3.^\circ394$ to the ecliptic plane. The orbit of Mars possesses an eccentricity of 0.09337 and an inclination of $1.^\circ850$; the argument of perigee is

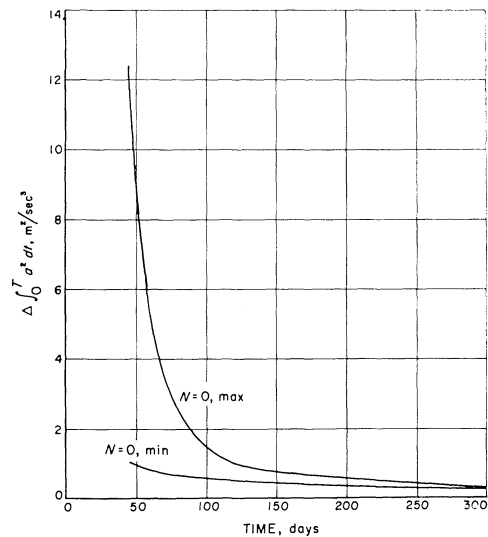


Fig. 8 Venus three-dimensional rendezvous trajectories, the effect of orbital inclination

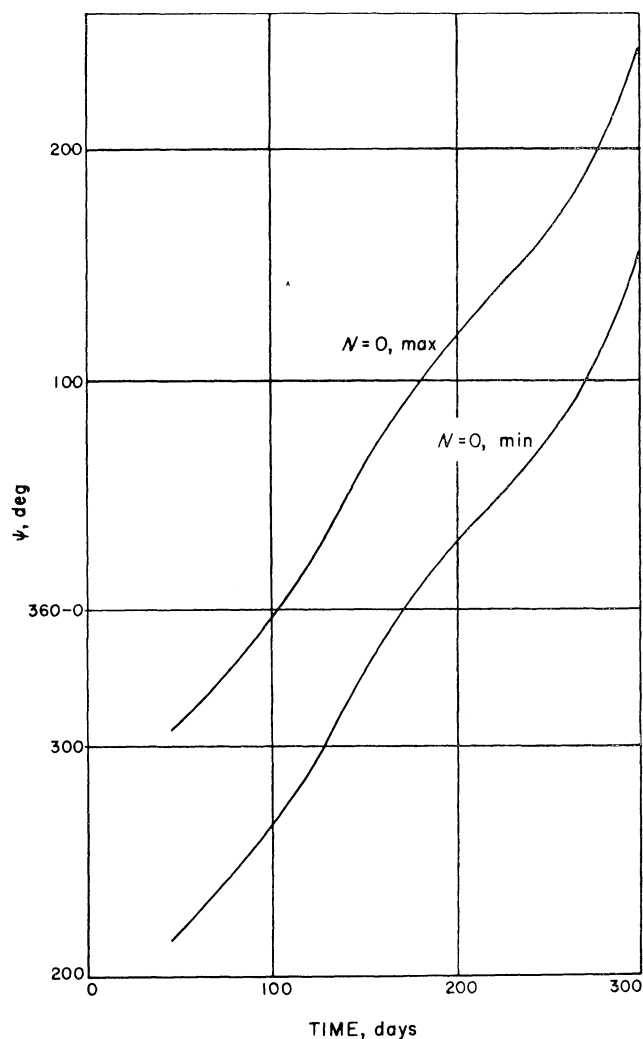


Fig. 9 Venus three-dimensional rendezvous trajectories, variation of positions of extremal points with flight time

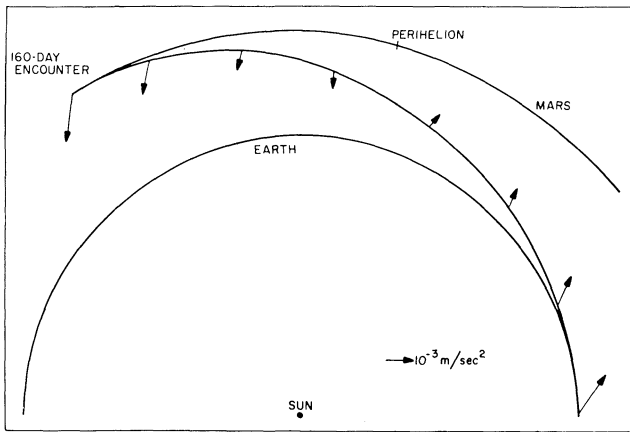


Fig. 10 Mars three-dimensional optimum rendezvous trajectory, ecliptic projection

-73.°93. The planets themselves were assumed massless, and only the mass of the sun was used in the calculations.

Fig. 3 illustrates an ecliptic projection of an interplanetary trajectory which will rendezvous Venus in 120 days. The terminal conditions in combination V were used. The arrows represent the ecliptic projection of \mathbf{a} at various points along the trajectory. Fig. 4 shows the variation of celestial latitude of the vehicle along this trajectory; the thrust program is presented in Fig. 5. The rendezvous of this particular trajectory is at the optimum point on Venus's orbit, which for this flight time is $\phi = -3.°189$ on the ascending branch. Because of symmetry, the point $\phi = +3.°189$ on the descending branch is also optimum. Fig. 6 exhibits the variation in the value of $\int_0^{t_1} a^2 dt$ and the transversality quantity $N(t_1)$, with rendezvous at different points along the orbit of Venus. $M(t_1)$ is zero at all rendezvous points in the case of Venus because of the circular terminal orbit. For this case the terminal conditions are given by combination V with condition 6 replaced by ψ_s . It is observed that the zero crossings of N mark the minimum and maximum values of $\int_0^{t_1} a^2 dt$ with respect to ψ . The amplitude of the variation is only a small percentage of the average value.

The iterative routine mentioned above was used to generate a series of two- and three-dimensional Venus trajectories for a wide range of flight times. Fig. 7 shows the variation in $\int_0^{t_1} a^2 dt$ for a two-dimensional model. The effect of the third dimension due to the inclination of Venus's orbit is exhibited by Fig. 8, in which the increment in $\int_0^{t_1} a^2 dt$ over the two-dimensional value has been plotted. Both the upper and lower bounds of this increment are included. The variation in ψ for both of these cases is shown in Fig. 9.

In ballistic interplanetary trajectories where velocity impulses are made at the terminal points, it is known that the effects of planetary inclinations on the required velocity increment to perform a mission can be quite severe. It will be observed, however, that this is not the case for advanced propulsion trajectories in which thrust is applied over an extended range. The reason for the comparatively slight effects of inclination is partly due to the small planetary inclinations involved and the relative efficiency with which the advanced system is capable of generating these required inclinations at the terminal point.

Orbital eccentricity has a considerably more prominent effect on $\int_0^{t_1} a^2 dt$, particularly for nearby planets such as Mercury and Mars. As a second example, a similar series of

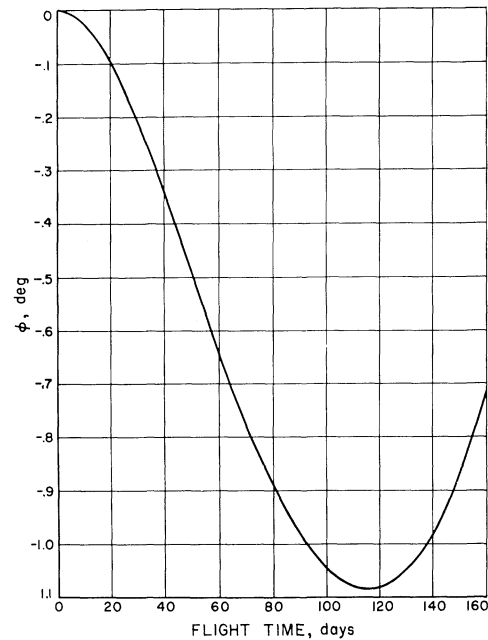


Fig. 11 Mars three-dimensional optimum rendezvous trajectory, celestial latitude

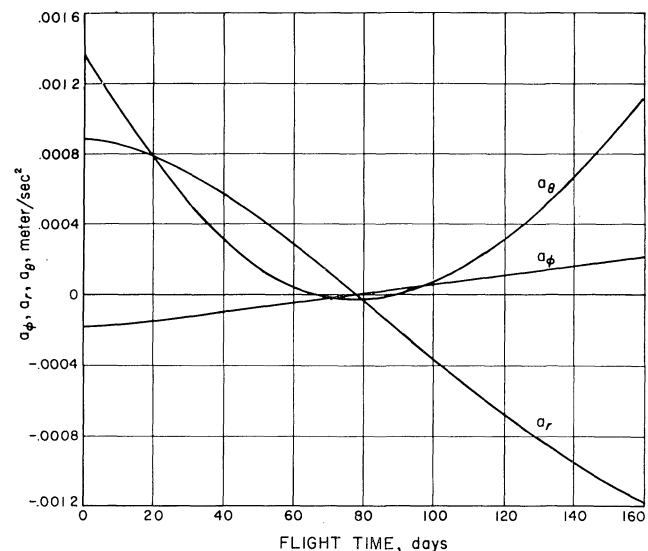


Fig. 12 Mars three-dimensional optimum rendezvous trajectory, thrust program

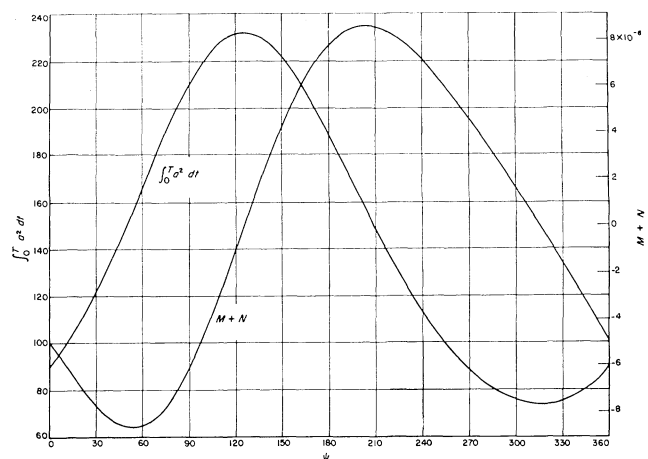


Fig. 13 Mars three-dimensional rendezvous trajectories, 90-day flight time

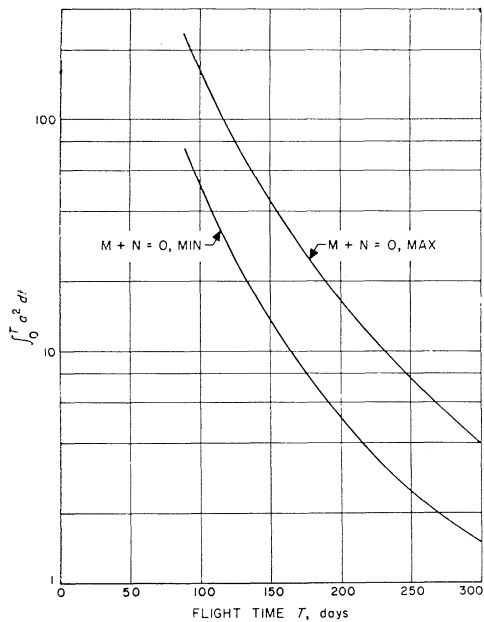


Fig. 14 Mars three-dimensional trajectories, rendezvous at extremal points

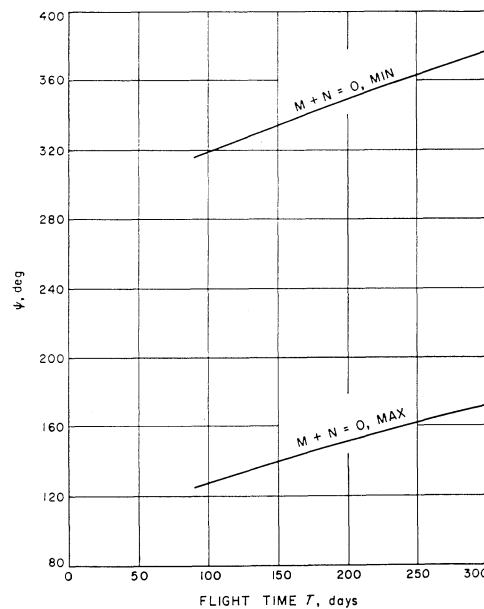


Fig. 15 Mars three-dimensional rendezvous trajectories, variations of positions of extremal points with flight time

results for rendezvous trajectories to Mars is presented. Figs. 10, 11, and 12 exhibit the characteristics of a 160-day trajectory which, for this flight time, will rendezvous at the optimum point on the orbit of Mars. The terminal conditions in combination III were used. Fig. 13 shows the effect of orbital eccentricity for a set of 90-day rendezvous trajectories to Mars. The magnitude of the variation of $\int_0^{t_1} a^2 dt$ with ψ is about 50% of the average value. The transversality expression $M(t_1) + N(t_1)$ is included, and its zero crossings coincide with the maximum and the minimum values of $\int_0^{t_1} a^2 dt$ with respect to ψ .

Fig. 14 shows the variation of $\int_0^{t_1} a^2 dt$ with flight time for both extremal points. The variation of these extremal points with flight time is shown in Fig. 15. As in the case of Venus, the effect of the inclination of the orbit of Mars is quite small. The contribution of inclination to the variation, $\int_0^{t_1} a^2 dt$ in Fig. 13, is less than 1% of the mean value. This was confirmed by a comparison with an analogous set of two-dimensional trajectories.

For interplanetary mission studies with advanced propulsion systems, it appears that planetary inclinations are negligible in payload capability studies. Even for the planet Mercury, with its 7° inclination, the effect is small.

On the other hand, the effect of orbital eccentricities warrants the use of the appropriate eccentric orbits for Mercury and Mars. In (2) a comparison of results obtained from using both circular and eccentric terminal orbits will be found.

Acknowledgment

The author wishes to express his sincere appreciation to D. E. Richardson (JPL), who collaborated in the development of the computer program for these calculations, and to G. C. Sauer (JPL), who made valuable contributions to discussions concerning the analysis.

This paper presents the results of one phase of research carried out at the Jet Propulsion Laboratory, California Institute of Technology, under Contract No. NASw-6, sponsored by NASA.

References

- 1 Irving, J., *Space Technology*, John Wiley and Sons Inc., New York, 1959, Chap. 10.
- 2 Melbourne, W. G., "Interplanetary Trajectories and Payload Capabilities of Advanced Propulsion Vehicles," *Tech. Rep. no. 32-68*, Jet Propulsion Laboratory, Pasadena, Calif., 1961.
- 3 Melbourne, W. G. and Sauer, C. G., Jr., "Optimum Thrust Programs for Power-Limited Propulsion Systems," *Tech. Rep. no. 32-118*, Jet Propulsion Laboratory, Pasadena, Calif., 1961.